

DYNAMICS OF POLYDISPERSE IRREVERSIBLE ADSORPTION: A PHARMACOLOGICAL EXAMPLE

RADEK ERBAN^{*,†,§}, S. JONATHAN CHAPMAN^{*}, KERRY D. FISHER[†],
IOANNIS G. KEVREKIDIS[‡] and LEONARD W. SEYMOUR[†]

^{}Mathematical Institute, University of Oxford,
24-29 St. Giles, Oxford OX1 3LB, UK
[§]erban@maths.ox.ac.uk*

*[†]Department of Clinical Pharmacology, University of Oxford,
Radcliffe Infirmary, Woodstock Road,
Oxford OX2 6HE, UK*

*[‡]Princeton University, Department Of Chemical Engineering,
PACM & Mathematics, Engineering Quadrangle, Olden Street,
Princeton, NJ 08544, USA*

Received 6 February 2006

Revised 9 August 2006

Communicated by N. Bellomo

Many drug delivery systems suffer from undesirable interactions with the host immune system. It has been experimentally established that covalent attachment (irreversible adsorption) of suitable macromolecules to the surface of the drug carrier can reduce such undesirable interactions. A fundamental understanding of the adsorption process is still lacking. In this paper, the classical random irreversible adsorption model is generalized to capture certain essential processes involved in pharmacological applications, allowing for macromolecules of different sizes, partial overlapping of the tails of macromolecules, and the influence of reactions with the solvent on the adsorption process. Working in one dimension, an integro-differential evolution equation for the adsorption process is derived, and the asymptotic behavior of the surface area covered and the number of molecules attached to the surface are studied. Finally, equation-free dynamic renormalization tools are applied to study the asymptotically self-similar behavior of the adsorption statistics.

Keywords: Random sequential adsorption; polydispersity; polymer coating.

AMS Subject Classification: 92C50, 05B40, 60K40

1. Introduction

Random sequential adsorption (RSA) is a classical model for various physical, chemical, and biological problems.⁷ In the simplest form, RSA processes can be formulated as sequential addition to a structure of objects that cannot overlap, and once inserted, cannot move or leave the structure.¹ In this paper, we present a pharmacological example in which application of the RSA model can provide meaningful

qualitative insights. Motivated by pharmacological applications, we present a slight generalization of the classical RSA model to enable us to study the effects of polydispersity and partial overlap of adsorbing macromolecules on the surface of a virus. We also study the dependence of the adsorption process on interactions (reactions) of the adsorbing macromolecules with the solvent.

The paper is organized as follows. In Sec. 2, we will introduce the motivating pharmacological example and our questions of interest. In Sec. 3, we will introduce the generalized random sequential adsorption (gRSA) model suitable for capturing essential features of the pharmacological problem from Sec. 2, which we formulate in one dimension. The analytical results for this model are presented in Sec. 4. We derive the governing integro-differential equation for the evolution of gaps between adsorbed polymers, and compute the asymptotic properties of the quantities of interest, namely the number of macromolecules adsorbed and the total area (in one dimension, length) they cover. In Sec. 5, we apply equation-free methods to the computational study of the system. The main idea that underlies this equation-free computer-assisted analysis is the design and execution of appropriately initialized short bursts of stochastic simulations; the results of these are processed to estimate coarse-grained quantities of interest — in this case the self-similarly evolving shape of the gap statistics in the problem. Finally, we summarize our conclusions in Sec. 6.

2. Pharmacological Background

Many medical conditions such as cancer, heart disease, and heritable disorders (hemophilia, cystic fibrosis, muscular dystrophy, etc.) have faulty, mutant genes as an underlying cause. Healthy, normal genes can be readily synthesized in the laboratory but introducing them into diseased cells remains a challenge. Many research groups are studying viruses, such as adenovirus, as a means to introduce normal genes into diseased cells. For therapeutic use, the virus' own DNA is usually partially or completely replaced by the gene of interest. The most common adenovirus strain used for this purpose is adenovirus type 5 (Ad5), because it is easy to manipulate and is non-pathogenic in humans.¹⁶ Ad5 has been used with great success to treat diseases in laboratory animals, but the results have not been replicated in humans. One of the greatest problems with using Ad5 in humans is the presence of neutralizing antibodies. In addition, the viruses often infect non-target cells, particularly the liver, causing unwanted toxicity. Our laboratory is exploring the use of reactive hydrophilic polymers based on poly [N-(2-hydroxypropyl) methacrylamide] (pHPMA) to coat virus particles and protect them from neutralizing antibodies by steric shielding. This technique is very effective at protecting the virus and permitting it to be retargeted to specific cell types.^{8,9,14} The polymer has multiple esters along its length that are used to bind to the amino side chain of lysine residues on the virus surface. In a coating reaction, the polymers bind randomly to the virus surface until (a) all of the lysine residues are occupied or (b) lysine residues are rendered inaccessible (obscured) by polymer chains. We know little about the orientation of

polymers on the virus surface or how to optimize the coating reaction because there are no techniques to visualize the orientation of polymers on the virus surface.

Representative questions one would like to answer are: How many polymer molecules will become attached to the viral surface by a given time? How large is the surface area covered by the polymer coat at that time? In this paper, a theoretical approach is chosen to address these questions for simplified models of the adsorption process. Since the adsorption process is driven by the diffusion of molecules to the surface of the virus, and since the adsorption is effectively irreversible, a suitable modification of the classical RSA might be applied to model the process. It is important to take into account polydispersity in the polymer size. Even if we prepare the polymer molecules with a specified target molecular weight, some relatively small molecules of the polymer will always be present, and they will diffuse faster than the larger molecules. A smaller molecule can reach the surface of the virus at a higher rate. We will consider the adsorption of polymers whose diameters are distributed according to a probability distribution function $P(z)$. The solution is assumed to be well mixed. We also define $p(z)$ as the probability distribution function of the particles which can reach the surface in a single time step. An important modeling issue lies in a good choice of $P(z)$ (e.g., it might be the Gamma distribution) and in a realistic relation between $P(z)$ and $p(z)$. In Sec. 3, we simply specify $p(z)$ (avoiding the above questions which are addressed in our subsequent publications^{5,6}). The long term dynamics of the polydisperse adsorption depends on the behavior of $p(z)$ close to zero. We will use different distributions $p(z)$ given by (3.1).

Finally, the reactive groups of the polymer molecules can also react with the solvent before reaching the surface. This is the case for commonly used biocompatible pHPMA reactive polymers.¹⁷ If all reactive groups of a polymer are already hydrolyzed, then the polymer cannot covalently bind to the surface of the virus. Hence, we have to consider that only a fraction $r(t)$ of the polymers is still reactive at time t . Depending on the form of $r(t)$, different polymer coats may be created. This issue will be discussed in more detail in Sec. 4.4.

Polymers are long flexible molecules.⁴ The pHPMA polymer molecule has (one or more) reactive group(s) which can react with the primary amino groups on the viral surface. As a result, a polymer molecule becomes covalently (irreversibly) attached to the surface at a point. The rest of the polymer is not attached (unless another covalent bond is created), and it freely “wiggles” in the space above the viral surface. Having in mind that the “wiggling tail” does not perfectly shield the underlying surface, we generalize the classical RSA model to allow partial overlap of the adsorbing macromolecules, i.e. we allow some squeezing of the polymers.

Let $N(t)$ be the number of polymers attached to the surface at time t . Let $A(t)$ be the total area of the surface covered by adsorbed polymers at time t . Since we cover the surface by polymers of different sizes, there is no obvious relation between $A(t)$ and $N(t)$. However, both variables $A(t)$ and $N(t)$ are of practical interest as discussed below.

We cover the surface of the virus by polymers to protect it from unwanted interactions. Hence, the number $A(t)$ gives us a simple characterization of the area of the surface which is protected by the polymer coat. The unwanted interactions are not the only problem which one has to overcome in order to use viruses as a drug delivery system. Another important task is to retarget the virus to infect the cells of interest (e.g. cancer cells) via new receptors. Assuming that we put one “targeting” group per polymer molecule, the number of targeting molecules will be equal to $N(t)$.

If we considered the adsorption of same-size nonoverlapping objects of area a , then we would have $A(t) = aN(t)$. In our case, the adsorbing molecules have different sizes. There is no obvious relation between $A(t)$ and $N(t)$, and both quantities are of interest. In the following sections, we will present theoretical approaches to compute the time evolution of $A(t)$ and $N(t)$.

3. A Simple Generalization of Random Sequential Adsorption

Random sequential adsorption has been extensively studied during the last several decades.⁷ The theoretical work is more mature in one dimension with information in higher dimensions mostly coming from numerical simulations.¹² If we consider fixed size objects, then RSA usually starts from an empty surface and continues until the time when no further object can be placed, the so-called “jamming limit”. If the objects to be covered have spherical symmetry,¹⁵ then the coverage approaches the jamming limit as $t^{-1/d}$, where t is time and d is the dimension. The asymptotic behavior can be more complicated for objects of different shape.⁷

As argued in Sec. 2, polydispersity is often present in real systems. If we allow adsorbing particles (in one spatial dimension) of arbitrarily small length, then the coverage approaches the full coverage as $t \rightarrow \infty$. Relatively less is known for polydisperse adsorption. One-dimensional analytical results can be found in Ref. 12, where it is assumed that the attached polymers prevent binding of other polymer molecules that would overlap with them. In reality, the polymer molecules are stretching during the adsorption process, creating a polymer brush (for semitelechelic polymers) after sufficiently long time.^{3,13} Thus, each molecule “covers” a smaller surface area at later times. Consequently, it is possible to adsorb more molecules onto the surface. Here, we take this fact into account, and we modify the random sequential adsorption algorithm accordingly. We state our generalized random sequential algorithm (gRSA) in one dimension as follows.

gRSA algorithm. *We consider adsorption of small intervals of different sizes onto the interval $[0, 1]$, the adsorbing domain. At each time step, the size of a small interval is chosen randomly according to the probability distribution function $p(z)$. We select randomly the position of its center w inside the adsorbing domain $[0, 1]$, and we make an attempt to place the small interval of length z there. If the center w of the segment to be*

adsorbed lies inside a segment already placed, the adsorption is rejected. If the position of the center w is chosen in the gap (x_1, x_2) between attached polymers, then the new polymer segment is adsorbed with probability $\xi(z, w - x_1, x_2 - w)$, where $w - x_1$ and $x_2 - w$ are distances of the center w of the polymer from the endpoints of the gap (x_1, x_2) .

The parameters of gRSA which have to be specified include the probability distribution function $p(z)$ and the probability $\xi(z, w - x_1, x_2 - w)$. In what follows, we assume that the lengths of polymers are distributed according to the formula

$$p(z) = \begin{cases} (\alpha + 1)\varepsilon^{-\alpha-1}z^\alpha & \text{for } z < \varepsilon, \\ 0 & \text{for } z \geq \varepsilon \end{cases} \quad (3.1)$$

for $\alpha > -1$ and small $\varepsilon \ll 1$. Let us assume that the position of the center w of the new polymer is chosen in the gap $[x_1, x_2]$, i.e. $w \in [x_2, x_1]$. Then we take the probability (per unit time) of adsorbing the polymer segment of length $z \leq x = x_2 - x_1$ as

$$\xi(z, w - x_1, x_2 - w) = \begin{cases} \frac{2(w - x_1)}{z} & \text{for } w \in \left[x_1, x_1 + \frac{z}{2}\right]; \\ 1 & \text{for } w \in \left[x_1 + \frac{z}{2}, x_2 - \frac{z}{2}\right]; \\ \frac{2(x_2 - w)}{z} & \text{for } w \in \left[x_2 - \frac{z}{2}, x_2\right]; \end{cases} \quad (3.2)$$

and the probability of adsorbing the polymer segment of length $z > x$ as

$$\xi(z, w - x_1, x_2 - w) = \begin{cases} \frac{2(w - x_1)}{z} & \text{for } w \in \left[x_1, \frac{x_1 + x_2}{2}\right]; \\ \frac{2(x_2 - w)}{z} & \text{for } w \in \left[\frac{x_1 + x_2}{2}, x_2\right]. \end{cases} \quad (3.3)$$

In the latter case, the maximum probability of adsorption is achieved for $w = \frac{x_1 + x_2}{2}$, for which $\xi(w) = \frac{x}{z}$. The formulas (3.2) and (3.3) give the same probability density function $\xi(\cdot)$ for $z = x$ as is desirable. The plot of ξ as a function of w is given in Fig. 1. Formula (3.2) is shown in Fig. 1(a), where the gap size $x = x_2 - x_1$ is greater

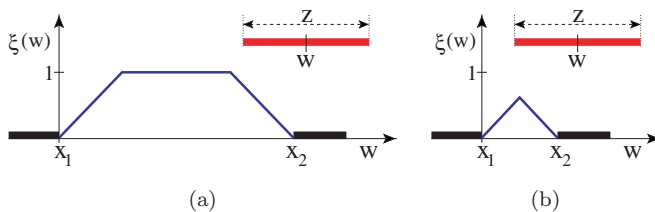


Fig. 1. The probability ξ as a function of w for gRSA model (3.2) and (3.3): (a) for the case $z \leq x = x_2 - x_1$; (b) for the case $z > x = x_2 - x_1$.

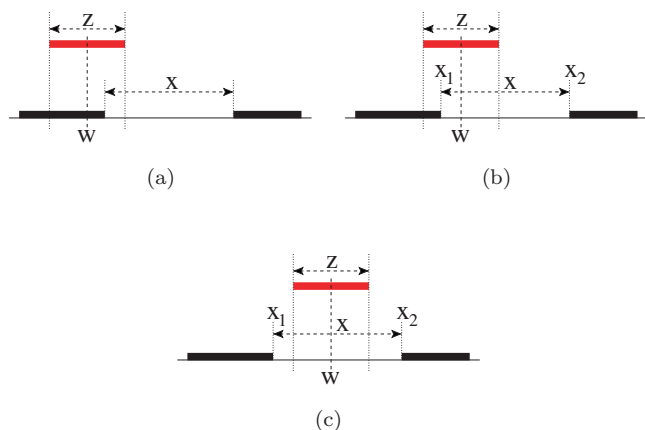


Fig. 2. Schematic of gRSA. (a) Polymer is refused; (b) polymer is adsorbed with probability $\xi(z, w - x_1, x_2 - w)$; (c) polymer is adsorbed.

than the length of the new polymer segment z . Formula (3.3) is shown in Fig. 1(b), where the gap size $x = x_2 - x_1$ is less than the length of the new polymer z .

To explain the motivation behind formula (3.2), three possible cases of the relative position of the new interval of the length $z \leq x$ (shown at the top of each panel) and the gap (x_1, x_2) are shown in Fig. 2. In Fig. 2(a), the new interval is rejected because its middle point w lies inside a polymer segment which is already adsorbed on the surface. Hence, the probability of adsorption is 0, the same probability as in the classical RSA model. In Fig. 2(c), the new segment of the length z does not overlap with neighboring polymers, and we allow it to be adsorbed with probability $\xi = 1$. Cases in Figs. 2(a) and 2(c) are treated as in the classical RSA model.

In Fig. 2(b), the center of the new polymer is inside the gap, but the new polymer overlaps with neighboring polymer segments. This polymer would be rejected by the classical RSA model. We believe it is more realistic to consider that such a polymer will be adsorbed with some nonzero probability which continuously interpolates between the cases shown in Figs. 2(a) and 2(c), i.e. between zero for $w - x_1 = 0$ and 1 for $w - x_1 = z$. Formula (3.2) takes this fact into account, using simple linear interpolation. Formula (3.3) naturally extends formula (3.2) for polymer segment lengths greater than the gaps (see also Fig. 1).

Having explained the new rules for adsorbing the polymer, we must also specify what part of the surface is actually covered. We will assume that the new polymer covers only the intersection of the intervals

$$\left[w - \frac{z}{2}, w + \frac{z}{2}\right] \cap [x_1, x_2]. \quad (3.4)$$

This guarantees that a possibly long, newly adsorbed polymer will not “spill over” and cover any part of the neighboring gaps.

4. Analysis of gRSA

Let $G(x, t)$ be the concentration of gaps (holes) of length x at time t , and let $C(x, t)$ be the corresponding cumulative probability distribution function; that is,

$$C(x, t) = \frac{1}{\int_0^\infty G(y, t) dy} \int_0^x G(y, t) dy. \quad (4.1)$$

The total length of the surface that is covered by polymers at time t , $A(t)$, is directly related to $G(x, t)$ by

$$A(t) = 1 - \int_0^1 x G(x, t) dx. \quad (4.2)$$

The number of polymers attached to the surface at time t , $N(t)$, can be also related to $G(x, t)$, as we will see in Sec. 4.1. Thus, the starting point of the analysis of the system is the derivation of the evolution equation for the distribution function of gaps $G(x, t)$.

A gap of length x can be created from a larger gap (of length $y > x$) by adsorbing a suitable interval to the system. Thus, the evolution of the concentration of gaps $G(x, t)$ is given by the equation

$$\begin{aligned} \frac{\partial G}{\partial t}(x, t) = & -G(x, t) \int_0^\infty \left[\int_0^x \xi(z, u, x-u) du \right] p(z) dz \\ & + \int_x^\infty \left[\int_0^{2(y-x)} 2\xi\left(z, x + \frac{z}{2}, y - x - \frac{z}{2}\right) p(z) dz \right] G(y, t) dy. \end{aligned} \quad (4.3)$$

Let us note that the transition from the discrete gRSA algorithm to the continuous description given by (4.3) would be exact if we averaged over (infinitely) many realizations of the adsorption process. Later, we show that analytical results derived from (4.3) are in good agreement with the results obtained by a single realization too. The successful application of the continuous description is possible because the size of the adsorbing polymers is small (less than ε) compared to the size of the adsorbing domain $[0, 1]$. Using (3.2) and (3.3), Eq. (4.3) can be rewritten in the following form:

$$\begin{aligned} \frac{\partial G}{\partial t}(x, t) = & -G(x, t) \int_0^x \left[\int_0^{z/2} \frac{2u}{z} du + \int_{z/2}^{x-z/2} 1 du + \int_{x-z/2}^x \frac{2(x-u)}{z} du \right] p(z) dz \\ & - G(x, t) \int_x^\infty \left[\int_0^{x/2} \frac{2u}{z} du + \int_{x/2}^x \frac{2(x-u)}{z} du \right] p(z) dz \\ & + \int_x^\infty \int_0^{y-x} 2G(y, t) p(z) dz dy \\ & + \int_x^\infty \int_{y-x}^{2(y-x)} 2 \frac{2(y-x) - z}{z} G(y, t) p(z) dz dy. \end{aligned} \quad (4.4)$$

Hence,

$$\begin{aligned}\frac{\partial G}{\partial t}(x, t) = & -G(x, t) \int_0^x \left[x - \frac{z}{2}\right] p(z) dz - G(x, t) \int_x^\infty \left[\frac{x^2}{2z}\right] p(z) dz \\ & + \int_x^\infty \int_0^{y-x} 2G(y, t) p(z) dz dy \\ & + \int_x^\infty \int_{y-x}^{2(y-x)} 2 \left[\frac{2(y-x)}{z} - 1\right] G(y, t) p(z) dz dy.\end{aligned}\quad (4.5)$$

We assume that the lengths of polymers are distributed according to formula (3.1) for $\alpha > -1$ and small $\varepsilon \ll 1$. Moreover, we assume that there are already no holes of length greater than $\varepsilon/2$ in the system, i.e. $G(x, t) = 0$ for $x > \varepsilon/2$. Then (using (3.1)), Eq. (4.5) can be rewritten (for $x < \varepsilon/2$ and $\alpha \neq 0$) as

$$\begin{aligned}\frac{\partial G}{\partial t}(x, t) = & -\frac{G(x, t)(\alpha + 1)}{\varepsilon^{\alpha+1}} \int_0^x \left[x - \frac{z}{2}\right] z^\alpha dz - \frac{G(x, t)(\alpha + 1)}{\varepsilon^{\alpha+1}} \int_x^\varepsilon \left[\frac{x^2}{2z}\right] z^\alpha dz \\ & + \frac{2(\alpha + 1)}{\varepsilon^{\alpha+1}} \int_x^\infty G(y, t) \int_0^{y-x} z^\alpha dz dy \\ & + \frac{2(\alpha + 1)}{\varepsilon^{\alpha+1}} \int_x^\infty G(y, t) \int_{y-x}^{2(y-x)} \left[\frac{2(y-x)}{z} - 1\right] z^\alpha dz dy,\end{aligned}$$

which implies

$$\begin{aligned}\frac{\partial G}{\partial t}(x, t) = & \frac{x^{\alpha+2}G(x, t)}{\alpha(\alpha + 2)\varepsilon^{\alpha+1}} - \frac{x^2G(x, t)(\alpha + 1)}{2\alpha\varepsilon} \\ & + \frac{2^{\alpha+2} - 4}{\alpha\varepsilon^{\alpha+1}} \int_x^\infty G(y, t)(y - x)^{\alpha+1} dy.\end{aligned}\quad (4.6)$$

If $\alpha = 0$, Eq. (4.5) implies (for $x < \varepsilon/2$)

$$\frac{\partial G}{\partial t}(x, t) = -\frac{x^2G(x, t)}{2\varepsilon} \left(\frac{3}{2} + \ln \left[\frac{\varepsilon}{x}\right]\right) + \frac{4 \ln 2}{\varepsilon} \int_x^\infty G(y, t)(y - x) dy. \quad (4.7)$$

Equation (4.6) (or (4.7)) is the desired integro-differential equation for $G(x, t)$. If we solve (4.6), we can compute the evolution of $A(t)$ by (4.2). The equation for the evolution of $N(t)$ is given in the next section.

4.1. Evolution of $N(t)$

At each time step, an interval of length between $(z, z + dz)$ is chosen with probability $p(z)dz$. This interval can be placed in any gap of size x with probability $\int_0^x \xi(z, u, x - u) du$. There exist $G(x, t)dx$ gaps whose size lies in the interval $(x, x + dx)$. Hence, the integral $\int_0^\infty [\int_0^x \xi(z, u, x - u) du] G(x, t) dx$ gives the probability that the randomly

chosen position of the polymer of length z will be accepted. Thus, the probability of attaching a polymer of any length at one time step is equal to

$$\int_0^\infty \int_0^\infty \left[\int_0^x \xi(z, u, x-u) du \right] G(x, t) p(z) dx dz. \quad (4.8)$$

Using a continuous approximation for $N(t)$, we find that $N(t)$ satisfies the following ordinary differential equation:

$$\frac{dN}{dt} = \int_0^\infty \int_0^\infty \left[\int_0^x \xi(z, u, x-u) du \right] G(x, t) p(z) dz dx. \quad (4.9)$$

Taking $p(z)$ to be given by (3.1) and $\xi(z, u, x-u)$ to be given by (3.2) and (3.3), and considering the regime where all gaps are already less than ε (i.e. $G(x, t) = 0$ for $x > \varepsilon$), we obtain

$$\begin{aligned} & \int_0^\infty \int_0^\infty \left[\int_0^x \xi(z, u, x-u) du \right] G(x, t) p(z) dz dx \\ &= \int_0^\infty \int_0^x \left[\int_0^{z/2} \frac{2u}{z} du + \int_{z/2}^{x-z/2} 1 du + \int_{x-z/2}^x \frac{2(x-u)}{z} du \right] G(x, t) p(z) dz dx \\ &+ \int_0^\infty \int_x^\infty \left[\int_0^{x/2} \frac{2u}{z} du + \int_{x/2}^x \frac{2(x-u)}{z} du \right] G(x, t) p(z) dz dx \\ &= \int_0^\varepsilon G(x, t) \int_0^x \left[x - \frac{z}{2} \right] p(z) dz dx + \frac{1}{2} \int_0^\varepsilon G(x, t) x^2 \int_x^\infty \frac{p(z)}{z} dz dx \\ &= \frac{\alpha+1}{\varepsilon^{\alpha+1}} \int_0^\varepsilon G(x, t) \int_0^x \left[x - \frac{z}{2} \right] z^\alpha dz dx + \frac{\alpha+1}{2\varepsilon^{\alpha+1}} \int_0^\varepsilon G(x, t) x^2 \int_x^\varepsilon z^{\alpha-1} dz dx \\ &= -\frac{1}{\alpha(\alpha+2)\varepsilon^{\alpha+1}} \int_0^\varepsilon G(x, t) x^{\alpha+2} dx + \frac{\alpha+1}{2\alpha\varepsilon} \int_0^\varepsilon G(x, t) x^2 dx. \end{aligned}$$

Hence

$$\frac{dN}{dt} = -\frac{1}{\alpha(\alpha+2)\varepsilon^{\alpha+1}} \int_0^\varepsilon G(x, t) x^{\alpha+2} dx + \frac{\alpha+1}{2\alpha\varepsilon} \int_0^\varepsilon G(x, t) x^2 dx. \quad (4.10)$$

Before analyzing (4.6) and (4.10) further, we summarize some results from the literature on the classical RSA.

4.2. Some results for the classical RSA

If we consider particles of the same length ε so that $p(z) = \delta(z - \varepsilon)$, and if we choose $\xi(z, w - x_1, x_2 - w)$ of the form

$$\xi(z, w - x_1, x_2 - w) = \begin{cases} 1 & \text{for } x_1 + \frac{z}{2} \leq w \leq x_2 - \frac{z}{2}, \\ 0 & \text{otherwise,} \end{cases} \quad (4.11)$$

then our gRSA algorithm reduces to the classical RSA algorithm. The evolution Eq. (4.3) can be used to verify known one-dimensional results about fixed segment

size, non-overlapping random sequential adsorption,¹² namely one can show that the jamming limit is asymptotically approached¹⁵ as t^{-1} .

Random sequential adsorption with a probability distribution $p(z)$ given by (3.1) and probability $\xi(z, w - x_1, x_2 - w)$ given by (4.11) has been studied in Ref. 12. Then Eq. (4.3) for $x < \varepsilon$ reads as follows (assuming that initially there exist no holes of length greater than ε in the system, i.e., $G(x, t) = 0$ for $x > \varepsilon$):

$$\frac{\partial G}{\partial t}(x, t) = -\frac{x^{\alpha+2}G(x, t)}{(\alpha+2)\varepsilon^{\alpha+1}} + \frac{2}{\varepsilon^{\alpha+1}} \int_x^{x+\varepsilon} G(y, t)(y-x)^{\alpha+1} dy. \quad (4.12)$$

The scaling ansatz¹² for the concentration $G(x, t)$ can be written as

$$G(x, t) \sim t^a \Phi(xt^b) \quad \text{for } x \ll 1, \quad t \gg 1 \quad \text{and} \quad xt^b \text{ finite.} \quad (4.13)$$

Defining the moments

$$M_\gamma(t) = \int_0^\infty x^\gamma G(x, t) dx, \quad m_\gamma = \int_0^\infty \xi^\gamma \Phi(\xi) d\xi \quad (4.14)$$

and using (4.13), we obtain

$$M_\gamma(t) \sim t^{a-b-b\gamma} m_\gamma. \quad (4.15)$$

Moreover, multiplying Eq. (4.12) by x^γ and integrating over x , one can derive the equation for moments,

$$\frac{\partial M_\gamma}{\partial t} = \frac{F(\gamma, \alpha)}{\varepsilon^{\alpha+1}} M_{\gamma+\alpha+2}, \quad \text{where } F(\gamma, \alpha) = 2B(\gamma+1, \alpha+2) - \frac{1}{\alpha+2}, \quad (4.16)$$

where $B(\cdot, \cdot)$ is the Beta function. We define the function $\hat{\gamma}(\alpha)$ implicitly by the equation $F(\hat{\gamma}, \alpha) = 0$. If γ is equal to $\hat{\gamma}(\alpha)$, then the moment M_γ is independent of time. Hence, using (4.15), we obtain the relation $a = b + b\hat{\gamma}(\alpha)$ between the coefficients of the scaling ansatz (4.13) and the parameter α of the model. Finally, substituting the scaling ansatz (4.13) in (4.12), we find that $b = (\alpha+2)^{-1}$. Thus, the scaling of moments (4.15) can be rewritten in the form

$$M_\beta(t) \sim t^\mu, \quad \text{where } \mu = \frac{\hat{\gamma}(\alpha) - \beta}{\alpha+2}. \quad (4.17)$$

Using (4.2) and (4.17), we obtain

$$1 - A(t) = \int_0^1 xG(x, t) dx \sim t^{-\omega(\alpha)}, \quad \text{where } \omega(\alpha) = \frac{1 - \hat{\gamma}(\alpha)}{\alpha+2}. \quad (4.18)$$

The graph of the function $\omega(\alpha)$ is given in Fig. 3(a). Equation (4.9) for $p(z)$ given by (3.1) and probability $\xi(z, w - x_1, x_2 - w)$ given by (4.11) reads as follows:

$$\frac{dN}{dt} = \frac{\varepsilon^{-\alpha-1}}{\alpha+2} \int_0^\varepsilon x^{\alpha+2} G(x, t) dx. \quad (4.19)$$

Using (4.17), we obtain (for $\sigma(\alpha) > 0$)

$$N(t) \sim t^{\sigma(\alpha)}, \quad \text{where } \sigma(\alpha) = \frac{\hat{\gamma}(\alpha)}{\alpha+2}. \quad (4.20)$$

The graph of the function $\sigma(\alpha)$ is given in Fig. 3(b).

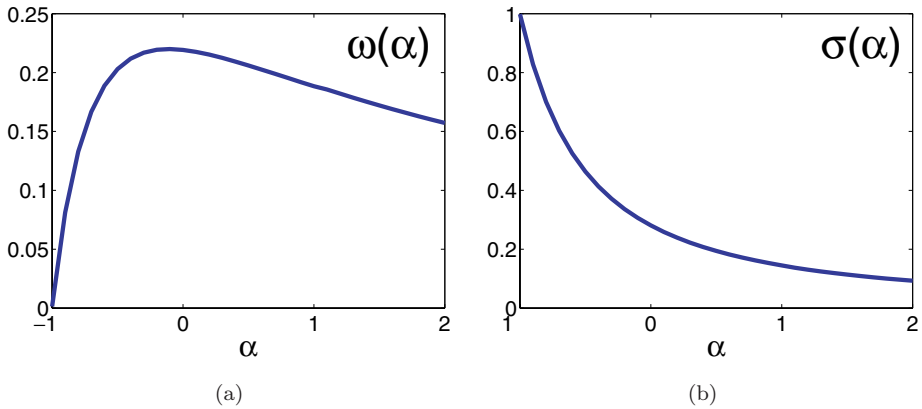


Fig. 3. (a) The graph of the exponent $\omega(\alpha)$ given by (4.18). (b) The graph of the exponent $\sigma(\alpha)$ given by (4.20).

4.3. Evolution of gRSA

The temporal evolution of the gRSA model is more complex than the cases discussed in Sec. 4.2. To see this, we use the moments $M_\gamma(t)$ defined by (4.14). Let us denote by $C(t)$ the maximal size of a gap in the system at time t . Clearly, $C(t) \rightarrow 0$ as $t \rightarrow \infty$. Moreover, we have the following inequality for the moments:

$$M_{\gamma_1}(t) = \int_0^\infty x^{\gamma_1 - \gamma_2} x^{\gamma_2} G(x, t) dx \leq C(t)^{\gamma_1 - \gamma_2} M_{\gamma_2}(t) \quad (4.21)$$

for any real numbers γ_1, γ_2 satisfying $\gamma_1 > \gamma_2$. Multiplying Eq. (4.6) by x^γ and integrating over x , we can derive the equation for moments (for $\alpha \neq 0$),

$$\begin{aligned} \frac{\partial M_\gamma}{\partial t} &= \frac{1}{\alpha(\alpha+2)\varepsilon^{\alpha+1}} M_{\gamma+\alpha+2} - \frac{\alpha+1}{2\alpha\varepsilon} M_{\gamma+2} \\ &\quad + \int_0^\infty \frac{2^{\alpha+2} - 4}{\alpha\varepsilon^{\alpha+1}} \int_x^\infty G(y, t) x^\gamma (y-x)^{\alpha+1} dy dx \\ &= \frac{1}{\alpha(\alpha+2)\varepsilon^{\alpha+1}} M_{\gamma+\alpha+2} - \frac{\alpha+1}{2\alpha\varepsilon} M_{\gamma+2} \\ &\quad + \int_0^\infty \frac{2^{\alpha+2} - 4}{\alpha\varepsilon^{\alpha+1}} G(y, t) \int_0^y x^\gamma (y-x)^{\alpha+1} dx dy \\ &= \frac{M_{\gamma+\alpha+2}}{\alpha(\alpha+2)\varepsilon^{\alpha+1}} + \frac{2^{\alpha+2} - 4}{\alpha\varepsilon^{\alpha+1}} \int_0^\infty G(y, t) y^{\gamma+\alpha+2} dy \int_0^1 \xi^\gamma (1-\xi)^{\alpha+1} d\xi \\ &\quad - \frac{\alpha+1}{2\alpha\varepsilon} M_{\gamma+2} \\ &= \frac{1}{\varepsilon^{\alpha+1}} \left(\frac{2^{\alpha+2} - 4}{\alpha} B(\gamma+1, \alpha+2) + \frac{1}{\alpha(\alpha+2)} \right) M_{\gamma+\alpha+2} - \frac{\alpha+1}{2\alpha\varepsilon} M_{\gamma+2} \\ &= \frac{1}{\varepsilon^{\alpha+1}} H(\gamma, \alpha) M_{\gamma+\alpha+2} - \frac{\alpha+1}{2\alpha\varepsilon} M_{\gamma+2}, \end{aligned} \quad (4.22)$$

where $B(\cdot, \cdot)$ is the Beta function and $H(\gamma, \alpha)$ is defined as

$$H(\gamma, \alpha) = \frac{2^{\alpha+2} - 4}{\alpha} B(\gamma + 1, \alpha + 2) + \frac{1}{\alpha(\alpha + 2)}. \quad (4.23)$$

First, consider the case $\alpha < 0$; inequality (4.21) implies that the dominant term on the right-hand side of (4.22) is the term $\varepsilon^{-\alpha-1} H(\gamma, \alpha) M_{\gamma+\alpha+2}$. The zeroth order moment,

$$M_0(t) = \int_0^\infty G(x, t) dx,$$

gives the total number of gaps at time t . At leading order, we have

$$\frac{\partial M_0}{\partial t} = \varepsilon^{-\alpha-1} H(0, \alpha) M_{\alpha+2}. \quad (4.24)$$

There is a constant $\bar{\alpha} \doteq -0.415$ such that $H(0, \alpha)$ is positive for $\alpha < \bar{\alpha}$ and negative for $\alpha > \bar{\alpha}$. We immediately see that, for $\alpha > \bar{\alpha}$ $M_0(t)$ is a decreasing nonnegative function of time. Moreover, we conclude that $M_0(t) \rightarrow 0$, i.e.

$$\lim_{t \rightarrow \infty} \int_0^\infty G(x, t) dx = 0 \quad \text{for } \alpha > \bar{\alpha}. \quad (4.25)$$

To see this, one can use (4.22) for $-1 < \gamma_0 < 0$. If negative γ_0 is sufficiently close to zero, then one concludes (in a manner similar to (4.24)) that $\partial M_{\gamma_0} / \partial t$ is negative. Consequently, M_{γ_0} is a bounded function. Using inequality (4.21) for $\gamma_1 = 0$ and $\gamma_2 = \gamma_0$, we obtain (4.25).

To illustrate result (4.25), we will execute two stochastic simulations with the gRSA algorithm. We will use (3.1)–(3.3) where $\alpha = -0.1$ or $\alpha = -0.3$. We choose $\varepsilon = 10^{-3}$. The results are given in Fig. 4, where the time evolution of the number of gaps and the number of adsorbed polymers are shown. Note that we use a logarithmic scale on the time axis because the long-term dynamics are very slow. For $\alpha = -0.1$, the stochastic simulation was stopped when 99.9999% of the surface was covered. For $\alpha = -0.3$, the stochastic simulation was stopped when 99.9994% of the surface was covered.

Next, we will study the behavior of the system for $\alpha < \bar{\alpha}$. Here, we will assume the scaling ansatz (4.13). Differentiating (4.23) with respect of γ , we obtain

$$\frac{\partial H}{\partial \gamma}(\gamma, \alpha) = \frac{2^{\alpha+2} - 4}{\alpha} B(\gamma + 1, \alpha + 2) [\psi_0(\gamma + 1) - \psi_0(\gamma + \alpha + 3)], \quad (4.26)$$

where ψ_0 is the polygamma function. For each $\alpha < \bar{\alpha}$, the equation

$$H(\bar{\gamma}, \alpha) = 0 \quad (4.27)$$

defines implicitly the function $\bar{\gamma}(\alpha)$. If γ is equal to $\bar{\gamma}(\alpha)$, then the moment M_γ is independent of time. Hence, using (4.15), we obtain the relation

$$a = b + b \bar{\gamma}(\alpha)$$

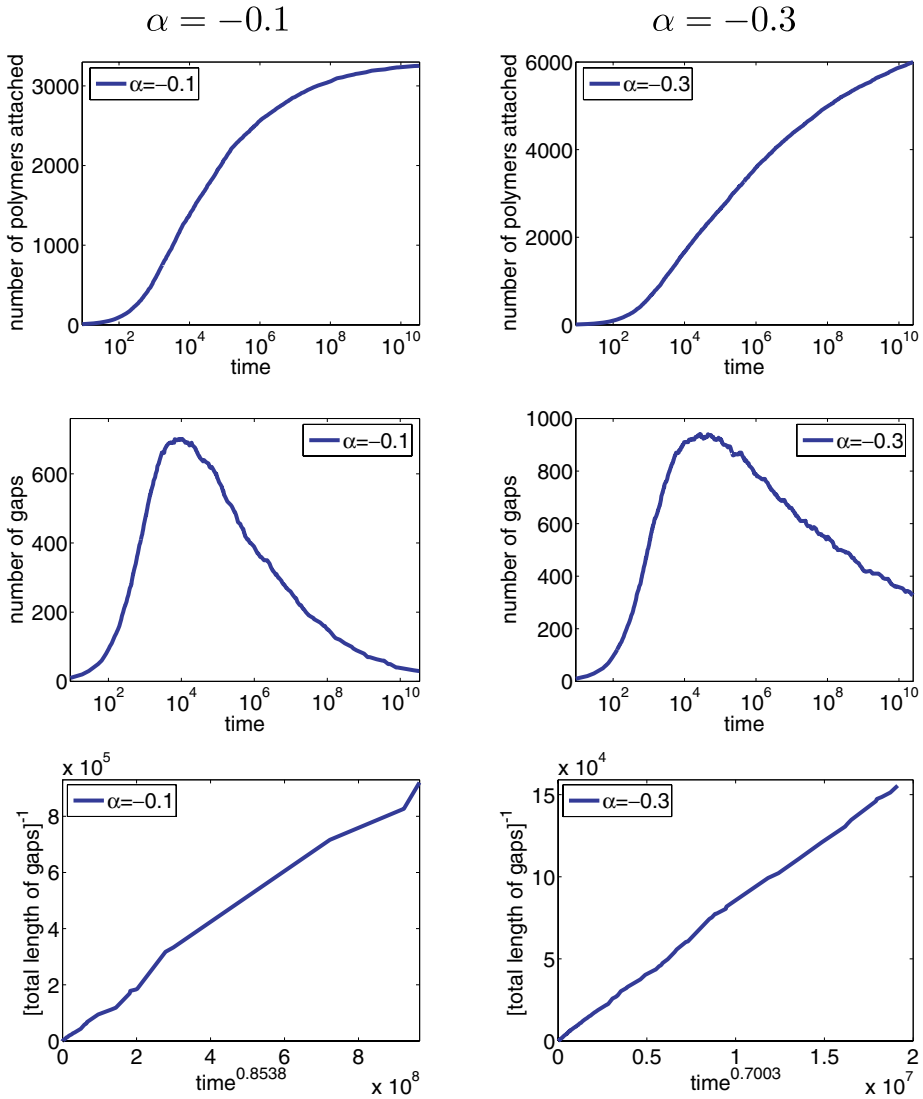


Fig. 4. gRSA model for $\alpha = -0.1$ (panels on the left) and $\alpha = -0.3$ (panels on the right). We plot the time evolution of the number of adsorbed polymers (top panels) and the time evolution of the number of gaps (middle panels). The time axis of the top and middle panels is logarithmic. We also plot the time evolution of the quantity $[1 - A(t)]^{-1}$ (bottom panels), where time is scaled according to (4.29).

between the coefficients of the scaling ansatz (4.13) and the parameter α of the model. Finally, substituting the scaling ansatz (4.13) into (4.22), one can find that $b = (\alpha + 2)^{-1}$. Hence, the scaling of moments (4.15) can be rewritten in the form

$$M_\beta(t) \sim t^{\bar{\mu}}, \quad \text{where } \bar{\mu} = \frac{\bar{\gamma}(\alpha) - \beta}{\alpha + 2}. \quad (4.28)$$

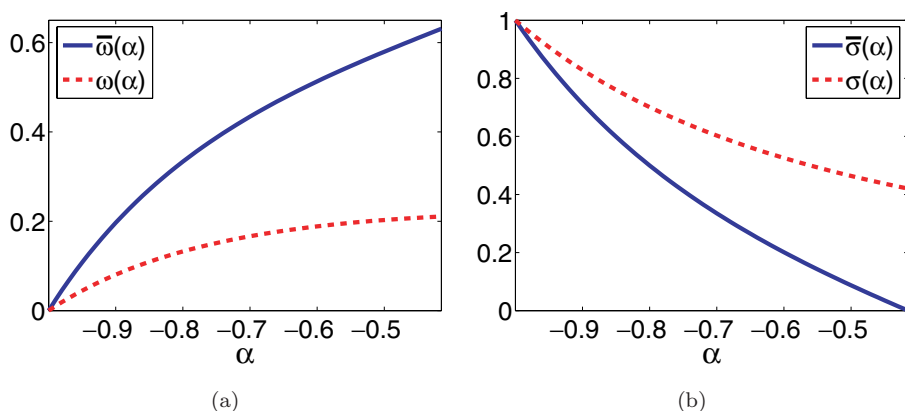


Fig. 5. (a) The graph of the exponent $\bar{\omega}(\alpha)$ given by (4.29). The dashed line shows the exponent $\omega(\alpha)$ given by (4.18). (b) The graph of the exponent $\bar{\sigma}(\alpha)$ given by (4.30). The dashed line shows the exponent $\sigma(\alpha)$ given by (4.20).

Using (4.2) and (4.28), we obtain

$$1 - A(t) = \int_0^1 xG(x, t)dx \sim t^{-\bar{\omega}(\alpha)}, \quad \text{where } \bar{\omega}(\alpha) = \frac{1 - \bar{\gamma}(\alpha)}{\alpha + 2}. \quad (4.29)$$

The graph of the function $\bar{\omega}(\alpha)$ is given in Fig. 5(a). We also plot $\omega(\alpha)$ given by (4.18) for comparison. Using (4.10) and (4.28), we also obtain

$$N(t) \sim t^{\bar{\sigma}(\alpha)} \quad \text{where } \bar{\sigma}(\alpha) = \frac{\bar{\gamma}(\alpha)}{\alpha + 2}. \quad (4.30)$$

The graph of the function $\bar{\sigma}(\alpha)$ is given in Fig. 5(b); we also plot $\sigma(\alpha)$ given by (4.20) for comparison.

To illustrate results (4.29) and (4.30), we will execute two gRSA stochastic simulations. We will use (3.1)–(3.3), where $\alpha = -0.5$ or $\alpha = -2/3$. We choose $\varepsilon = 10^{-3}$. The results are given in Fig. 6 where the time evolution of the number of adsorbed polymers and the time evolution of (the inverse of) the total length of gaps are shown. The time is scaled according to (4.29) and (4.30); we solve (4.27) to obtain the desired exponents

$$\bar{\sigma}(-0.5) = 0.0872, \quad \bar{\omega}(-0.5) = 0.5795, \quad \bar{\sigma}\left(-\frac{2}{3}\right) = 0.2875, \quad \bar{\omega}\left(-\frac{2}{3}\right) = 0.4625, \quad (4.31)$$

and then we plot the results of stochastic simulations using the corresponding scaling (4.31). In Fig. 6, we also plot the cumulative distribution function $C(x, t)$ for different times (i.e., for different numbers of polymers attached). Using the suitable rescaling $\hat{C}(x, t) = C(kx, t)$, the curves collapse to a single curve as shown in Fig. 7.

Finally, one can easily show that formula (4.29) works also for the case $\bar{\alpha} \leq \alpha < 0$. To illustrate it, we plot the time evolution of the quantity $[1 - A(t)]^{-1}$ for

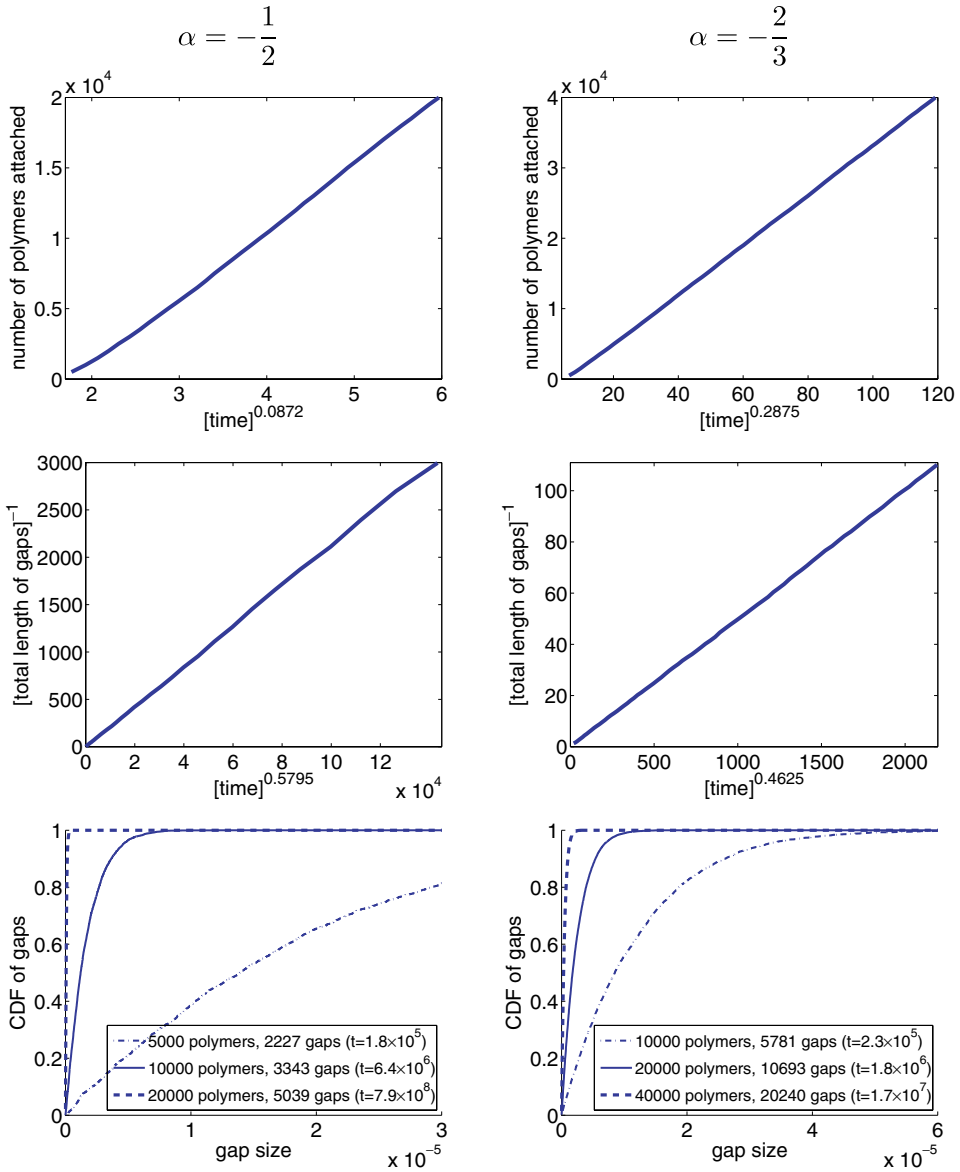


Fig. 6. gRSA model for $\alpha = -0.5$ (panels on the left) and $\alpha = -2/3$ (panels on the right). We plot the time evolution of the number of adsorbed polymers (top panels) and the time evolution of the inverse gap size $[1 - A(t)]^{-1}$ (middle panels). Time is scaled according to (4.31) (top and middle panels). We also plot the cumulative distribution function $C(x, t)$ at different times for both simulations (bottom panels).

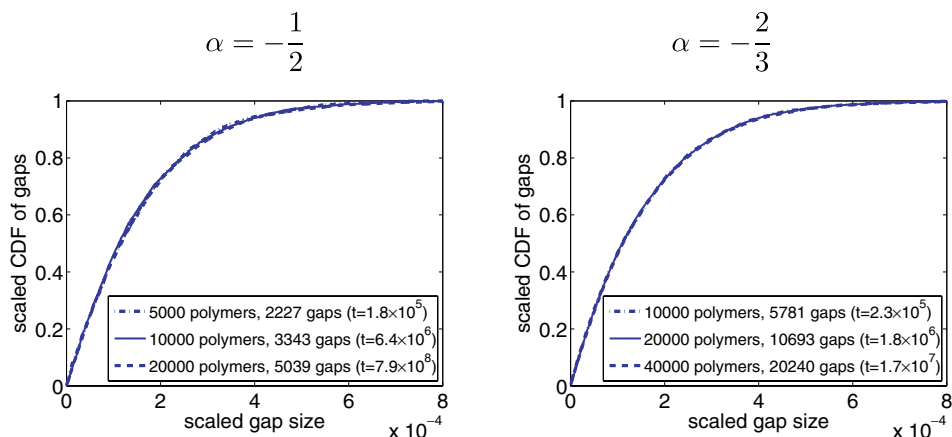


Fig. 7. Scaled cumulative distribution function of gaps for the gRSA model for $\alpha = -0.5$ (panel on the left) and $\alpha = -2/3$ (panel on the right).

$\alpha = -0.1$ and $\alpha = -0.3$ in Fig. 4 (bottom panel) using the scaling (4.29). On the other hand, formula (4.30) is no longer correct because integrating of (4.10) implies that $N(t)$ is approaching a constant value. More precisely, $N(t) \sim C + t^{\overline{\sigma}(\alpha)}$ for $\overline{\sigma}(\alpha) < 0$. If α is positive, then (4.25) is valid, i.e., we have (4.25) for any $\alpha > \overline{\alpha}$.

4.4. Time dependent concentration of reactive polymers

As discussed before, the reactive groups on our polymers are capable of reacting with the solvent before reaching the surface.¹⁷ It may therefore be more realistic to consider that only a fraction of polymers $r(t)$ is still reactive at time t . Here, $r(t) \in [0, 1]$, $r(0) = 1$, and $r(t)$ is a decreasing function of time.

The random sequential adsorption algorithm has to be modified as follows: at each time step, we generate a random number uniformly distributed in the interval $(0, 1)$. If this number is greater than $r(t)$, then the selected polymer has lost its binding site through reaction with the solvent (it cannot be adsorbed), and we continue with the next step. Otherwise, we choose randomly a position on the interval, and we attempt to place the polymer there.

Depending on the form of function $r(t)$, different dynamics can be observed. First, let us suppose that

$$r(t) = \frac{1}{t^\lambda} \quad \text{for } \lambda \in [0, 1). \quad (4.32)$$

In this case, we can find a relation between the modified random sequential algorithm and the previous results. At each time t , we can compute the average waiting time Δt before a reactive polymer hits the surface as the solution of the equation

$$\int_t^{t+\Delta t} \frac{1}{\tau^\lambda} d\tau = 1. \quad (4.33)$$

Solving (4.33), we find

$$(t + \Delta t)^{1-\lambda} = t^{1-\lambda} + 1 - \lambda.$$

Hence,

$$\Delta t = \left[t^{1-\lambda} + 1 - \lambda \right]^{1/(1-\lambda)} - t \sim t^\lambda.$$

Consequently, we can make use of the formulas (4.18) and (4.20), or formulas (4.29) and (4.30), in the case (4.32). For example, using (4.18) and (4.20), we obtain that the quantities $A(t)$ and $N(t)$ satisfy the following asymptotic behavior:

$$A(t) \sim t^{(1-\lambda)\omega(\alpha)} \quad \text{and} \quad N(t) \sim t^{(1-\lambda)\sigma(\alpha)}. \quad (4.34)$$

To illustrate formula (4.34), we stochastically simulate the gRSA model with the probability distribution $p(z)$ given by (3.1) and the probability $\xi(z, w - x_1, x_2 - w)$ given by (4.11), where the fraction of the reactive polymers in the system decreases with time according to (4.32). We select $\varepsilon = 10^{-3}$ and verify the asymptotic behavior (4.34) for $\alpha = -0.5$ and $\lambda = 0.5$. Then (4.34) implies

$$1 - A(t) \sim t^{-0.1014} \quad \text{and} \quad N(t) \sim t^{0.2319}.$$

The time evolution of $A(t)$ and $N(t)$ is given in Fig. 8 (top panels). We also present results for $\alpha = 0$ and $\lambda = 0.33$ in Fig. 8 (bottom panels). Again, we scale the time according to (4.34).

The reactive group is lost by chemical reaction with the solvent. It might be more natural to consider (instead of (4.32)) that the fraction of reactive polymers is exponentially decreasing, i.e.

$$r(t) = e^{-\lambda t} \quad \text{for } \lambda > 0. \quad (4.35)$$

Formula (4.35) gives rise to qualitatively different dynamics for the system, as opposed to the dynamics associated with (4.32). For simplicity, let us assume that every polymer with a functional reactive group can be adsorbed (which will give a bound on $N(t)$ from above). Then the average number of adsorbed polymers $N(t)$ is

$$N(t) = \frac{1}{\lambda} (1 - e^{-\lambda t}),$$

which implies that the number of adsorbed polymers does not approach infinity as in the previous case.

5. Equation-Free Analysis of gRSA

In the previous theory, we assumed the scaling ansatz (4.13) (see also Ref. 12) for $G(x, t)$, and we computed the time dependence of the quantities of interest $A(t)$ and $N(t)$. A related interesting question is whether we can also compute the profile Φ from (4.13). One possibility is to substitute (4.13) in Eq. (4.6) and solve it numerically for Φ , but we will not proceed this way. Instead, we demonstrate the

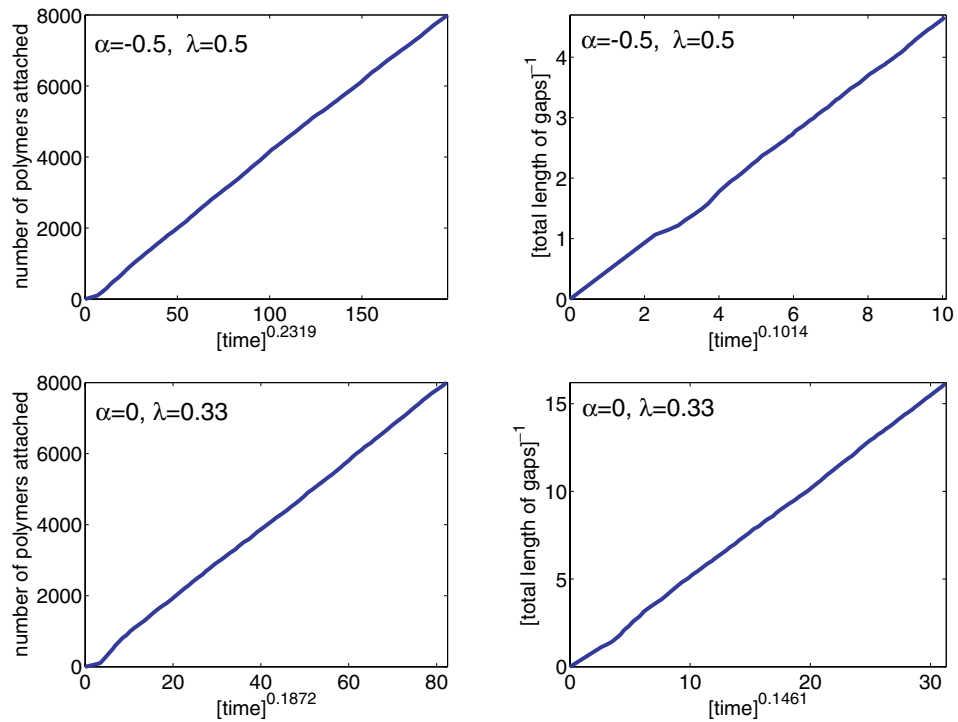


Fig. 8. Modified RSA model from Sec. 4.4. The time evolution of the number of polymer molecules attached to the surface $N(t)$ (left). Time evolution of the inverse of the total gap size $[1 - A(t)]^{-1}$ (right). Time is scaled according to (4.34).

computation of the self-similar profile Φ using only short-time appropriately initialized simulations of the stochastic gRSA model. In this equation-free context,^{11,2} it is easier to work with the cumulative distribution function $C(x, t)$, which can be obtained from $G(x, t)$ through (4.1); $C(x, t)$ is less noisy than $G(x, t)$ (e.g. see Ref. 10). Using (4.1) and (4.13), we obtain

$$\begin{aligned} C(x, t) &= \frac{1}{\int_0^\infty G(y, t) dy} \int_0^x G(y, t) dy \\ &= \frac{1}{\int_0^\infty \Phi(y t^b) dy} \int_0^x \Phi(y t^b) dy = \frac{1}{\int_0^\infty \Phi(\xi) d\xi} \int_0^{x t^b} \Phi(\xi) d\xi. \end{aligned}$$

Hence, we see that the cumulative density function $C(x, t)$ scales as

$$C(x, t) \equiv \overline{C}(x t^b). \tag{5.1}$$

To compute the profile \overline{C} , we can use an equation-free iterative fixed point algorithm which is shown schematically in Fig. 9. Starting with the initial guess \overline{C}_0 , we compute the sequence of profiles \overline{C}_K , $K = 1, 2, 3, \dots$, where

$$\overline{C}_{K+1} = \Psi(\overline{C}_K) \text{ for } K = 0, 1, 2, 3, \dots, \tag{5.2}$$

and where the mapping Ψ is obtained as the composition of the following four steps:

- Given the cumulative density profile \bar{C}_K , create one or more microscopic realizations of gaps in the unit interval such that the initial cumulative density function is $C(\cdot, 0) = \bar{C}_K$.
- Use the microscopic simulator (i.e. use the gRSA algorithm) for a short time Δt .
- Compute the new cumulative distribution function $C(\cdot, \Delta t)$ at time Δt .
- Rescale $C(\cdot, \Delta t)$ to compute \bar{C}_{K+1} .

One possible way to rescale $C(\cdot, \Delta t)$ is to compute the average gap size a_0 from $C(\cdot, 0)$ and the average gap size $a_{\Delta t}$ from $C(\cdot, \Delta t)$. Then \bar{C}_{K+1} can be computed by

$$\bar{C}_{K+1}(x) = C\left(\frac{a_{\Delta t}}{a_0}x, \Delta t\right). \quad (5.3)$$

We now present illustrative results obtained by this fixed point computation (5.2) using the gRSA algorithm. We will use (3.1)–(3.3), where $\alpha = -0.5$ or $\alpha = -2/3$. We choose $\epsilon = 10^{-3}$. The results of long-term simulations for these parameter values were already shown in Fig. 6. Our goal is to use the iterative formula (5.2) to compute the scaled cumulative distribution function profile which was shown in Fig. 7. This algorithm allows us to find the self-similar shape by performing simulations while simulating at a scale (at relatively larger average gap sizes) where the evolution is relatively fast, compared to the long-term dynamics close to jamming. The initial guess is given as

$$\bar{C}_0(x) = \begin{cases} 0 & \text{for } x \leq 1.5 \times 10^{-4}, \\ 1 & \text{for } x > 1.5 \times 10^{-4}, \end{cases}$$

which means that initially all our gaps have the same size 1.5×10^{-4} . At each iteration step (see Fig. 9), we place 1000 gaps according to the cumulative distribution function \bar{C}_K to the interval $[0, 1]$. We evolve the simulation until 100 new polymers are placed. We then *rescale* the new cumulative distribution according to (5.3), and we compute \bar{C}_{K+1} . Several iterations are shown in Fig. 10 (top panels). We see that after 20 iterations, we have effectively reached the steady state (the

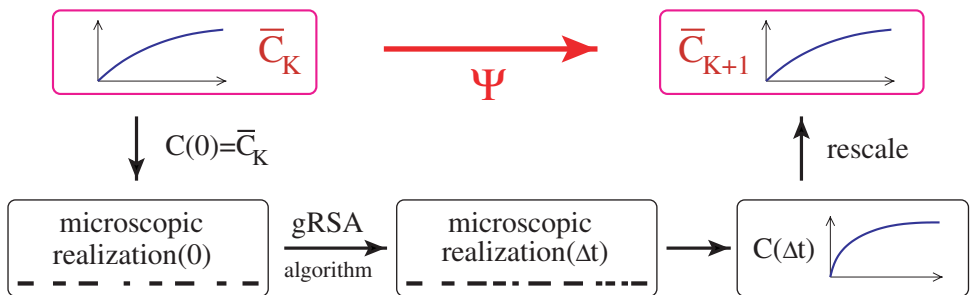


Fig. 9. Schematic of the equation-free mapping Ψ .

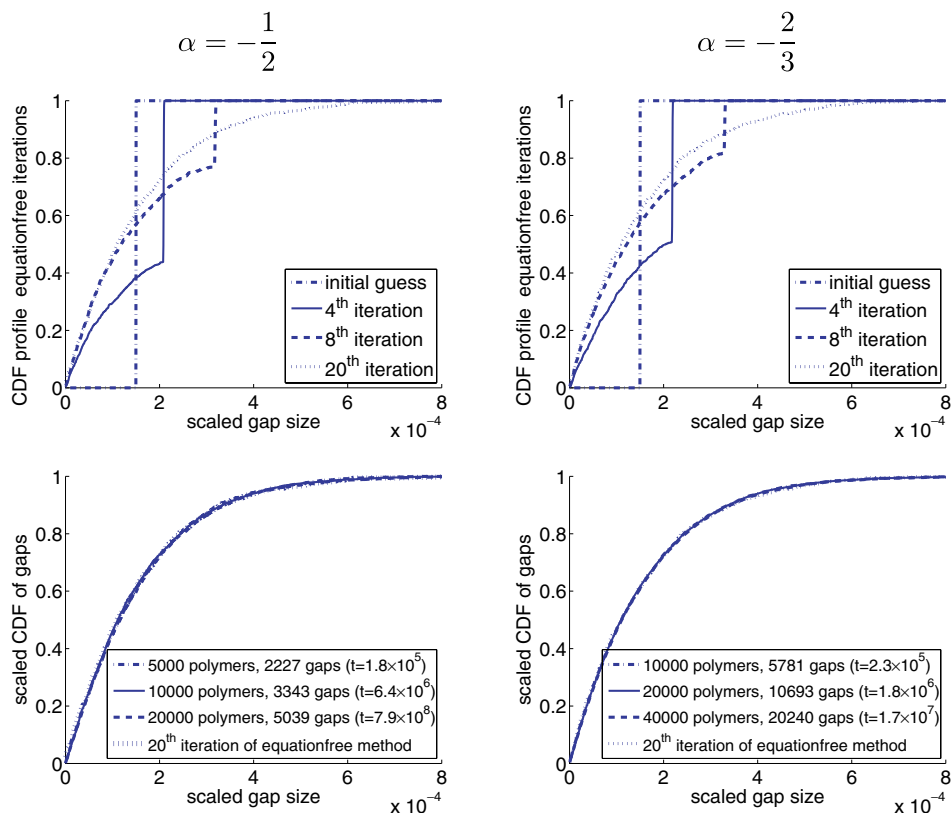


Fig. 10. Equation-free gRSA computational results for $\alpha = -0.5$ (left panels) and $\alpha = -2/3$ (right panels). Iterations of the equation-free dynamic renormalization algorithm (5.2) (top panels). Comparison with the steady state profile obtained through long time simulations (bottom panels).

stationary shape of the self-similarly evolving gap distribution). More precisely, the error between iterations is small, and it is not further systematically decreasing. The comparison of the equation-free 20th iteration with the results obtained by the long-time simulations are also shown in Fig. 10 (bottom panels).

Finally, we note that many other algorithmic possibilities for the computation of the profile \bar{C} exist. Equation (5.2) seeks a fixed point of the mapping Ψ . Instead of successive substitution, other fixed point algorithms implemented in a matrix-free fashion through short simulation bursts can be used to find stationary solutions — for example, Newton-GMRES iterations²; these would be able to converge on even dynamically unstable self-similarly evolving distributions.

6. Discussion

In this paper, motivated by a pharmacological example involving polymer coating of a virus surface, we studied certain aspects of polydisperse adsorption of

macromolecules in one spatial dimension. We presented an extension of the classical random sequential adsorption algorithm to better capture certain essential properties of the pharmacological model system currently used in drug development research. We introduced partial overlapping of adsorbing macromolecules, i.e., we considered that the polymers are not rigid objects, but they can be deformed while attaching to the surface. We found two distinct asymptotic regimes. Depending on the parameters of the processes involved, we can observe that either (a) the number of gaps between polymers asymptotically approaches zero, or that (b) the number of gaps asymptotes to infinity and the gap distribution acquires an asymptotically self-similar profile.

We also briefly discussed the impact of a possible reaction of the polymers with the solvent on gRSA dynamics. Again, two possibilities exist. If the decay of the reactive groups is relatively weak, then the dynamics of the system remains qualitatively unchanged and the system only evolves on a slower time scale. On the other hand, if the reactive groups decay exponentially, this decay ultimately wins over the polynomial time asymptotics of gRSA. From the application point of view, it therefore becomes crucial to know the corresponding rate constants in order to reliably predict what type of behavior one might expect over the time scales of interest. Typically, the coating process is performed overnight in the laboratory, and different reactive groups have different half lives; measuring these rates becomes an important task.

In this paper we worked in one spatial dimension and provided analytical results about the long time behavior of gRSA models. The analytical approach was based on two important facts: we knew what the good macroscopic observables for describing the system behavior were, and we were able to write down analytically tractable equations for these observables. The good observable for our system was a distribution of gaps $G(x, t)$ between adsorbed polymers. If we know the initial distribution of gaps $G(0, t)$, one could easily predict $G(x, t)$ at future times.

On the other hand, if we know (hope) that the gap distribution $G(x, t)$ is a good observable for the system of interest but we do not know the evolution equation for $G(x, t)$, then it is still possible to use the equation-free methods.¹¹ The main idea of the equation-free methods is to use the short bursts of appropriately initialized microscopic/stochastic computations to *estimate* macroscopic quantities of interest on demand. Hence, if an explicit coarse-grained evolution equation for the system statistics is not available, one can in principle avoid long, brute-force simulations. This might be the case for one-dimensional adsorption problems with more complicated microscopic evolution rules.

The situation becomes significantly more difficult in the higher dimensional case. Here, the analytical theory is far behind in development, and the literature contains mostly computational results. The first question for higher dimensional adsorption is the nature of the “good” coarse-grained observables for the system. Good observables (the variables in terms of which the unavailable effective model would be written) are necessary for developing a useful analytical theory. Knowing

appropriate coarse-grained observables is also an important feature of equation-free algorithms. Having one-dimensional analogues in mind, we see that one needs an effective way to describe the statistics of “gaps” (free space) in higher dimensions. If we cannot estimate (by intuition or by suitable algorithms for the detection of low-dimensionality in high-dimensional data) effectively good observables for the system, then the direct, brute-force computationally intensive simulations might be the only modeling option. In this paper we showed cases where we could do more than brute-force simulation and provided analytical results giving insights into the dynamics of gRSA.

The problems studied in this paper were motivated by the pharmacological example mentioned above, and realistic predictive modeling of the problem clearly requires extensive model parameter information that must come from experimental data. As we showed, we can expect different dynamics of the problem depending on the values of the parameters of the polymer and the virus which are used. Obtaining reliably such parameters and bounds on their uncertainty for our particular model problem is non-trivial, and we are not yet ready to report about it.

Acknowledgments

This work was supported by the Biotechnology and Biological Sciences Research Council (grant Ref. BB/C508618/1). I.G.K. gratefully acknowledges a Guggenheim fellowship.

References

1. N. Brilliantov, Y. Andrienko, P. Krapivsky and J. Kurths, Fractal formation and ordering in random sequential adsorption, *Phys. Rev. Lett.* **76** (1996) 4058–4061.
2. L. Chen, I. Kevrekidis and P. Kevrekidis, Equation-free dynamic renormalization in a glassy compaction model, *Phys. Rev. E* **74** (2006) 016702.
3. P. de Gennes, Conformations of polymers attached to an interface, *Macromolecules* **13** (1980) 1069–1075.
4. M. Doi, *Introduction to Polymer Physics* (Oxford Univ. Press, 1996).
5. R. Erban and S. J. Chapman, Reactive boundary conditions for stochastic simulations of reaction-diffusion processes, *Phys. Biol.* **4** (2007) 16–28.
6. R. Erban and S. J. Chapman, Time scale of random sequential adsorption, to appear in *Phys. Rev. E* (2007).
7. J. Evans, Random and cooperative sequential adsorption, *Rev. Mod. Phys.* **65** (1993) 1281–1329.
8. K. Fisher, Y. Stallwood, N. Green, K. Ulbrich, V. Mautner and L. Seymour, Polymer-coated adenovirus permits efficient retargeting and evades neutralising antibodies, *Gene Ther.* **8** (2001) 341–348.
9. K. Fisher, K. Ulbrich, V. Šubr, C. Ward, V. Mautner, D. Blakey and L. Seymour, A versatile system for receptor-mediated gene delivery permits increased entry of DNA into target cells, enhanced delivery to the nucleus and elevated rates of transgene expression, *Gene Ther.* **7** (2000) 1337–1343.
10. C. Gear, Projective integration methods for distributions, NEC TR 2001-130 (2001), pp. 1–9.

11. I. Kevrekidis, C. Gear, J. Hyman, P. Kevrekidis, O. Runborg and K. Theodoropoulos, Equation-free, coarse-grained multiscale computation: Enabling microscopic simulators to perform system-level analysis, *Commun. Math. Sci.* **1** (2003) 715–762.
12. P. Krapivsky, Kinetics of random sequential parking on a line, *J. Stat. Phys.* **69** (1992) 135–150.
13. S. Milner, T. Witten and M. Cates, Theory of the grafted polymer brush, *Macromolecules* **21** (1988) 2610–2619.
14. C. Pouton and L. Seymour, Key issues in non viral gene delivery, *Adv. Drug Deliv. Rev.* **34** (1998) 3–19.
15. R. Swendsen, *Dynamics of Random Sequential Adsorption*, *Phys. Rev. A* **24** (1981) 504–508.
16. S. Vorburger and K. Hunt, Adenoviral gene therapy, *Oncologist* **7** (2002) 46–59.
17. V. Šubr, Č. Koňák, R. Laga and K. Ulbrich, Coating of DNA/Poly(L-lysine) complexes by covalent attachment of poly[N-(2-hydroxypropyl)methacrylamide], *Biomacromol.* **7** (2006) 122–130.